

# Projectile Launch Point Estimation from Radar Measurements

Eric Nelson, Meir Pachter, and Stanton Musick

**Abstract**—Nonlinear regression with an intercept is investigated and a new nonlinear regression algorithm is developed. The application area considered is ballistic trajectory determination from battlefield radar measurements. Specifically, the geo-location of an enemy artillery piece is pursued. Careful modelling of the nonlinear measurement situation at hand and the inclusion of an intercept parameter in the nonlinear regression shows a considerable improvement over conventional iterative least squares estimation when nonlinearity is dominant. Moreover, the estimation performance does not degrade from standard iterative least squares (ILS) in cases where the nonlinearity is weak compared to the measurement noise in the equation error, provided that the data record is sufficiently long.

## I. INTRODUCTION

The benefits and potential applications of batch estimation using linear and/or nonlinear regression with the inclusion of an intercept are investigated. In [1], batch parameter estimation is used for the identification in real-time of the control derivatives of an aircraft with distributed effectors. In [2], a stochastic framework to rigorously derive a centralized Differential Global Positioning System estimation algorithm for a formation of air vehicles is developed. The users cooperatively estimate positions and velocities using batch nonlinear regression.

The reasons why one should consider batch regression for nonlinear problems include the need for a sufficiently large data set in order to obtain a useful parameter estimate. A physically significant time interval must elapse to capture the nonlinearity, which is conducive to a batch estimation approach. Second, in the nonlinear case where the extended Kalman Filter recursive estimation paradigm is employed, bad state estimates at the beginning of the recursion will diverge the filter. When an initial short data window is used, one fails to obtain proper excitation observability and poor estimates are produced. At the same time, large data sets used in batch estimation do not pose a problem. With large data sets, piecewise batch estimation and recombination algorithms are used, which rely on tractable matrix inversions. Finally, in our specific application of geolocating an artillery piece, we are interested in the initial state estimate. Batch

processing yields the initial state estimates directly, without the need for smoothing. Hence, we employ batch estimation and nonlinear regression.

In this paper, the novel idea is advanced of including an intercept parameter in the nonlinear regression equations in order to account for linearization induced truncation errors. This differs from [3], where on-line identification using linear regression is investigated for reconfigurable flight control using an intercept parameter that is introduced to capture offset/change in trim effects caused by failure. Finally, in previous work [4], two new methods that incorporate an intercept to account for unmodelled bias, are used to estimate the frequency of a sinusoidal waveform and its DC component. This paper extends the linear estimation theory developed in [3] and [4] into nonlinear regression. The current paper is an attack on nonlinearity by including an intercept parameter in nonlinear regression that accounts for linearization induced truncation error. It is shown that the estimation performance is enhanced, particularly when the nonlinearity is strong. Also, when the nonlinearity is weak, the results do not degrade from standard ILS.

## II. BALLISTIC TRAJECTORY TRACKING

To fix ideas, consider the kinematics of a ballistic trajectory. This application is relevant on today's battlefield, as demonstrated by the British armed forces recent acquisition [5] of the Mobile Artillery Monitoring Battlefield Radar (MAMBA). MAMBA is deployed to scan for and track enemy projectiles in order to geo-locate the enemy artillery position. We apply nonlinear regression to this estimation problem. The developed theory is also applicable to a variety of other applications, including satellite trajectory determination [6].

The ballistic trajectory is modelled using a kinematic model typically employed in fire control systems:

$$\begin{aligned}x(t) &= x_o + V_{x_o}t \\y(t) &= y_o + V_{y_o}t \\z(t) &= z_o + V_{z_o}t - \frac{1}{2}c_b g t^2\end{aligned}\tag{1}$$

where  $x_o$ ,  $y_o$ , and  $z_o$  are the launch point coordinates,  $V$  is the projectile's muzzle velocity, and  $c_b$  is the projectile ballistic coefficient. We do not know where the projectile is being fired from; hence, the objective of our nonlinear regression estimation. The unknown parameter vector is:

$$\theta = (x_o, y_o, z_o, V_{x_o}, V_{y_o}, V_{z_o})^T \in \mathbb{R}^6\tag{2}$$

We carefully model the measurement situation at hand and use nonlinear regression to estimate the parameter  $\theta$

The views expressed in this article are those of the author and do not reflect the official policy or position of the United States Air Force, Department of Defense, or the U.S. Government.

E. Nelson, Captain, U.S. Air Force, Air Force Institute of Technology, 2950 Hobson Way, Wright Patterson Air Force Base, OH 45433, USA [eric.nelson@afit.edu](mailto:eric.nelson@afit.edu)

M. Pachter is with the Department of Electrical and Computer Engineering, Air Force Institute of Technology, 2950 Hobson Way, Wright Patterson Air Force Base, OH 45433, USA [meir.pachter@afit.edu](mailto:meir.pachter@afit.edu)

S. Musick is with the Sensors Directorate, Air Force Research Laboratory, Wright Patterson Air Force Base, OH 45433, USA [stanton.musick@wpafb.af.mil](mailto:stanton.musick@wpafb.af.mil)

TABLE I  
NONDIMENSIONAL VARIABLES

$x_o \rightarrow \frac{x_o}{VT}$	$y_o \rightarrow \frac{y_o}{VT}$	$z_o \rightarrow \frac{z_o}{VT}$	$R \rightarrow \frac{R}{VT}$
$v_R \rightarrow \frac{v_R}{VT}$	$\sigma_R \rightarrow \frac{\sigma_R}{VT}$	$V_{x_o} \rightarrow \frac{x_o}{V}$	$V_{y_o} \rightarrow \frac{y_o}{V}$
$V_{z_o} \rightarrow \frac{z_o}{V}$	$\Delta T \rightarrow \frac{\Delta T}{T}$	$t \rightarrow \frac{t}{T}$	$c_b \rightarrow c_b \frac{gT}{V}$

to obtain the launch position. Also, to acquire a fix on projectile launch position, we assume knowledge of the delay in initiating the tracking and/or knowledge of launch point elevation.

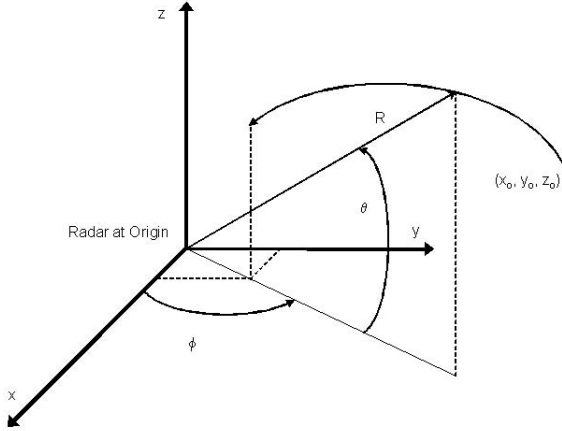


Fig. 1. Ballistic Trajectory Tracking Commences at  $(x_o, y_o, z_o)$ .

Radar measurements are comprised of range  $R$ , azimuth  $\phi$ , and elevation  $\theta$ . Without loss of generality, the radar is located at the origin, as shown in Figure 1. Perfect data satisfies the nonlinear measurement equations

$$R(t) = \sqrt{x^2(t) + y^2(t) + z^2(t)} \quad (3)$$

$$\tan(\phi(t)) = \frac{y(t)}{x(t)}$$

$$R(t) \sin(\theta(t)) = z(t)$$

At this point, we nondimensionalize all variables with the following scaling factors as appropriate:  $T$  represents the total duration of measurement and  $V$  represents the muzzle velocity of the projectile. Table I summarizes the nondimensionalized variables. Nondimensionalization improves the conditioning of the nonlinear regression process and estimation performance.

The trajectory is sampled. Considering (1) and (3), this implies that at a time  $t = k \Delta T$ :

$$R(k \cdot \Delta T) = \frac{y_o + V_{y_o} k \Delta T}{\sqrt{(x_o + V_{x_o} k \Delta T)^2 + (y_o + V_{y_o} k \Delta T)^2 + (z_o + V_{z_o} k \Delta T - \frac{1}{2} c_b k^2 \Delta T^2)^2}}$$

$$\tan(\phi(k \cdot \Delta T)) = \frac{y_o + V_{y_o} k \Delta T}{x_o + V_{x_o} k \Delta T}$$

$$R(k \Delta T) \cdot \sin(\theta(k \cdot \Delta T)) = z_o + V_{z_o} k \Delta T - \frac{1}{2} c_b k^2 \Delta T^2$$

where  $k = 0, 1, \dots, N-1$ . The recorded measurements are

$$R_m(k \cdot \Delta T) = R(k \cdot \Delta T) + v_R(k)$$

$$\phi_m(k \cdot \Delta T) = \phi(k \cdot \Delta T) + v_\phi(k)$$

$$\theta_m(k \cdot \Delta T) = \theta(k \cdot \Delta T) + v_\theta(k)$$

where the subscript  $m$  denotes the measurement variables and  $v_R$ ,  $v_\phi$ , and  $v_\theta$  are additive Gaussian white noise with variances  $\sigma_R$ ,  $\sigma_\phi$ , and  $\sigma_\theta$ .

### III. NONLINEAR REGRESSION

Consider the general nonlinear regression

$$Z = h(\theta) + W \quad (4)$$

where  $h(\theta)$  is the nonlinear observation relation and  $W$  is the equation error. In our application, the measurement vector is composed as follows:

$$Z_{N \times 1}^{(R)} \triangleq \begin{pmatrix} R_m(0) \\ R_m(\Delta T) \\ \vdots \\ R_m((N-1)\Delta T) \end{pmatrix}$$

$$Z_{N \times 1}^{(\phi)} \triangleq \begin{pmatrix} \tan(\phi_m(0)) \\ \tan(\phi_m(\Delta T)) \\ \vdots \\ \tan(\phi_m((N-1)\Delta T)) \end{pmatrix}$$

$$Z_{N \times 1}^{(R,\theta)} \triangleq \begin{pmatrix} R_m(0) \cdot \sin(\theta_m(0)) \\ R_m(\Delta T) \cdot \sin(\theta_m(\Delta T)) \\ \vdots \\ R_m((N-1)\Delta T) \cdot \sin(\theta_m((N-1)\Delta T)) \end{pmatrix}$$

and finally

$$Z_{(3N) \times 1} \triangleq \begin{pmatrix} Z^{(R)} \\ Z^{(\phi)} \\ Z^{(R,\theta)} \end{pmatrix}$$

Concerning the equation error, define:

$$V_{N \times 1}^{(R)} \triangleq \begin{pmatrix} v_R(0) \\ v_R(\Delta T) \\ \vdots \\ v_R((N-1)\Delta T) \end{pmatrix} \quad (5)$$

$$W_{N \times 1}^{(\phi)} \triangleq \begin{pmatrix} \frac{1}{1+\phi_m^2(0)} v_\phi(0) \\ \frac{1}{1+\phi_m^2(\Delta T)} v_\phi(\Delta T) \\ \vdots \\ \frac{1}{1+\phi_m^2((N-1)\Delta T)} v_\phi((N-1)\Delta T) \end{pmatrix}$$

$$W_{N \times 1}^{(R,\theta)} \triangleq \begin{pmatrix} \sin(\theta_m(0)) \cdot v_r(0) + R_m(0) \cos(\theta_m(0)) \cdot v_\theta(0) \\ \sin(\theta_m(\Delta T)) \cdot v_r(\Delta T) + R_m(\Delta T) \cos(\theta_m(\Delta T)) \cdot v_\theta(\Delta T) \\ \vdots \\ \sin(\theta_m((N-1)\Delta T)) \cdot v_r((N-1)\Delta T) + \dots \\ R_m((N-1)\Delta T) \cos(\theta_m((N-1)\Delta T)) \cdot v_\theta((N-1)\Delta T) \end{pmatrix}$$

where  $v_R(k \Delta T)$  is the range measurement error at time  $k \Delta T$ ,  $v_\phi(k \Delta T)$  is the azimuth measurement error at time

$k\Delta T$ , and  $v_\theta(k\Delta T)$  is the elevation measurement error at time  $k\Delta T$ . This yields the equation error vector

$$W_{(3N)\times 1} \triangleq \begin{pmatrix} V^{(R)}(\theta) \\ W^{(\phi)}(\theta) \\ W^{(R,\theta)}(\theta) \end{pmatrix}$$

We have obtained the explicit nonlinear regression in the parameter  $\theta = (x_o, y_o, z_o, V_{x_o}, V_{y_o}, V_{z_o})^T$ , which consists of the  $3N$  equations in (4).

Next, consider the measurement error vector.  $V_{N\times 1}^{(R)}$  is given in (5). In addition,

$$V_{N\times 1}^{(\phi)} \triangleq \begin{pmatrix} v_\phi(0) \\ v_\phi(\Delta T) \\ \vdots \\ v_\phi((N-1)\Delta T) \end{pmatrix}$$

and

$$V_{N\times 1}^{(\theta)} \triangleq \begin{pmatrix} v_\theta(0) \\ v_\theta(\Delta T) \\ \vdots \\ v_\theta((N-1)\Delta T) \end{pmatrix}$$

Therefore, we set

$$V_{(3N)\times 1} \triangleq \begin{pmatrix} V^{(R)} \\ V^{(\phi)} \\ V^{(\theta)} \end{pmatrix}$$

Finally, we define the  $N \times N$  diagonal matrices

$$D_N^{(\phi)} \triangleq \text{Diag} \left( \frac{1}{1 + \phi_m^2(k\Delta T)} \right)_{k=0}^{(N-1)}$$

$$D_N^{(\theta)} \triangleq \text{Diag} (\sin(\theta_m k\Delta T))_{k=0}^{(N-1)}$$

$$D_N^{(R,\theta)} \triangleq \text{Diag} (R_m(k\Delta T) \cdot \cos(\theta_m k\Delta T))_{k=0}^{(N-1)}$$

where the subscript  $m$  denotes measured variables. We compose the  $(3N) \times (3N)$  matrix

$$\Gamma_{(3N)\times(3N)} \triangleq \begin{bmatrix} I_N & 0 & 0 \\ 0 & D_N^{(\phi)} & 0 \\ D_N^{(\theta)} & 0 & D_N^{(R,\theta)} \end{bmatrix}$$

and we write the nonlinear regression (4) in the form

$$Z = h(\theta) + \Gamma V$$

where the equation error  $W = \Gamma V$ .

In the nonlinear regression (4), the equation error covariance is

$$R = E(W \cdot W^T)$$

Hence, we calculate

$$R = E \left( \begin{pmatrix} V_R & D_N^{(\phi)} \cdot V^{(\phi)} & D_N^{(\theta)} \cdot V^{(\theta)} + D_N^{(R,\theta)} \cdot V^{(\theta)} \\ D_N^{(\theta)} \cdot V^{(\theta)} + D_N^{(R,\theta)} \cdot V^{(\theta)} & \sigma_\phi^2 \cdot D_N^{(\phi)^2} & 0 \\ \sigma_R^2 \cdot I_N & 0 & \sigma_R^2 \cdot D_N^{(\theta)} \end{pmatrix} \right)$$

$$= \begin{bmatrix} \sigma_R^2 \cdot I_N & 0 & \sigma_R^2 \cdot D_N^{(\theta)} \\ 0 & \sigma_\phi^2 \cdot D_N^{(\phi)^2} & 0 \\ \sigma_R^2 \cdot D_N^{(\theta)} & 0 & \sigma_R^2 \cdot D_N^{(\theta)^2} + \sigma_\theta^2 \cdot D_N^{(R,\theta)^2} \end{bmatrix} \quad (6)$$

This assumes that range, azimuth, and elevation measurement noises are independent. Also, note that since  $R$  is symmetric, we only need  $R(1, 1)$ ,  $R(1, 2)$ ,  $R(1, 3)$ ,  $R(2, 2)$ ,  $R(2, 3)$ , and  $R(3, 3)$ .

Next, consider the nonlinear observation function  $h$  in (4). The following vectors are defined

$$h^{(R)}(\theta) \triangleq \begin{pmatrix} \sqrt{\frac{x_o^2 + y_o^2 + z_o^2}{(x_o + V_{x_o} \Delta T)^2 + (y_o + V_{y_o} \Delta T)^2 + (z_o + V_{z_o} \Delta T - \frac{1}{2} c_b \Delta T^2)^2}} \\ \vdots \\ \sqrt{\frac{x_o^2 + y_o^2 + z_o^2}{(x_o + V_{x_o} (N-1)\Delta T)^2 + (y_o + V_{y_o} (N-1)\Delta T)^2 + \dots}} \\ \frac{y_o + V_{y_o} (N-1)\Delta T}{(z_o + V_{z_o} (N-1)\Delta T - \frac{1}{2} c_b \Delta T^2 (N-1)^2)^2} \end{pmatrix}$$

$$h^{(\phi)}(\theta) \triangleq \begin{pmatrix} \frac{y_o}{x_o + V_{x_o} \Delta T} \\ \frac{y_o + V_{y_o} \Delta T}{x_o + V_{x_o} \Delta T} \\ \vdots \\ \frac{y_o + V_{y_o} \Delta T (N-1)}{x_o + V_{x_o} \Delta T (N-1)} \end{pmatrix}$$

$$h^{(R,\theta)}(\theta) \triangleq \begin{pmatrix} z_o + V_{z_o} \Delta T - \frac{1}{2} c_b \Delta T^2 \\ \vdots \\ z_o + V_{z_o} \Delta T (N-1) - \frac{1}{2} c_b \Delta T^2 (N-1)^2 \end{pmatrix}$$

and

$$h(\theta)_{(3N)\times 1} \triangleq \begin{pmatrix} h^{(R)}(\theta) \\ h^{(\phi)}(\theta) \\ h^{(R,\theta)}(\theta) \end{pmatrix}$$

We now linearize the observation equation for  $h(\theta)$ . Suppose  $\hat{\theta}^{(i)}$  is the current parameter estimate at step  $i$ . We linearize about  $\hat{\theta}^{(i)}$ . Let

$$H_i \triangleq \frac{\partial h}{\partial \theta} \Big|_{\theta=\hat{\theta}^{(i)}}$$

The regressor matrix  $H_i$  is composed as follows:

$$H_i = \begin{bmatrix} \frac{\partial h^{(R)}(\theta)}{\partial \theta} \Big|_{\theta=\hat{\theta}^{(i)}} \\ \frac{\partial h^{(\phi)}(\theta)}{\partial \theta} \Big|_{\theta=\hat{\theta}^{(i)}} \\ \frac{\partial h^{(R,\theta)}(\theta)}{\partial \theta} \Big|_{\theta=\hat{\theta}^{(i)}} \end{bmatrix}$$

where the parameter vector was specified in (2). The components for the linearized regressor are explicitly given in [7].

#### IV. STANDARD ILS ESTIMATION

Reconsider the general nonlinear regression (4). Expand the function  $h(\theta)$  about the current parameter estimate  $\hat{\theta}^{(k)}$  as follows:

$$h(\theta) = h(\hat{\theta}^{(k)}) + \theta - \hat{\theta}^{(k)}$$

$$= h(\hat{\theta}^{(k)}) + \frac{\partial h}{\partial \theta} \Big|_{\theta=\hat{\theta}^{(k)}} \cdot (\theta - \hat{\theta}^{(k)}) + r$$

where  $\hat{\theta}^{(k)}$  is the current parameter estimate and  $r$  is the truncation error.

$$h(\theta) = h(\hat{\theta}^{(k)}) + \frac{\partial h}{\partial \theta} \Big|_{\theta=\hat{\theta}^{(k)}} \cdot \theta - \frac{\partial h}{\partial \theta} \Big|_{\theta=\hat{\theta}^{(k)}} \hat{\theta}^{(k)} + r$$

Inserting this expansion into (4) yields

$$Z = h(\hat{\theta}^{(k)}) + \frac{\partial h}{\partial \theta} \Big|_{\theta=\hat{\theta}^{(k)}} \cdot \theta - \frac{\partial h}{\partial \theta} \Big|_{\theta=\hat{\theta}^{(k)}} \hat{\theta}^{(k)} + r + V$$

This implies

$$Z + H_k \cdot \hat{\theta}^{(k)} - h(\hat{\theta}^{(k)}) = H_k \cdot \theta + r + V$$

where

$$H_k \triangleq \frac{\partial h}{\partial \theta} \Big|_{\theta=\hat{\theta}^{(k)}}$$

In the conventional ILS approach, the presence of truncation error  $r$  is ignored. One considers

$$Z + H_k \cdot \hat{\theta}^{(k)} - h(\hat{\theta}^{(k)}) = H_k \cdot \theta + V$$

and iterates as in [6]:

$$\hat{\theta}^{(i+1)} = (H_i^T R^{-1} H_i)^{-1} H_i^T R^{-1} [Z + H_i \hat{\theta}^{(i)} - h(\hat{\theta}^{(i)})]$$

Also, note that at step  $i$ ,  $H_i$  is  $\hat{\theta}^{(i)}$  dependent. At the instant of convergence, where  $\hat{\theta}^{(i)} \rightarrow \hat{\theta}$  as  $i \rightarrow \infty$ , one calculates the parameter estimation error covariance matrix

$$P = (H_\infty^T R^{-1} H_\infty)^{-1}$$

Standard ILS performs very well, for example, in GPS.

Note that so far, the development is rather conventional, with the exception of the way that the measurements are treated in (3). During the iteration, and upon convergence, the strength of the nonlinearity in  $h$  is reduced using this formulation.

## V. NONLINEAR REGRESSION WITH INTERCEPT

We now augment the parameter vector and include an intercept into the nonlinear regression [4]. After linearization, the augmented formulation is

$$\begin{aligned} Z + H_i \cdot \hat{\theta}^{(i)} - h(\hat{\theta}^{(i)}) &= H_i \cdot \theta + e \cdot c + W' & (7) \\ &= \begin{bmatrix} H_i \\ e \end{bmatrix} \cdot \begin{bmatrix} \theta \\ \dots \\ c \end{bmatrix} + W' \\ &= \mathbf{H}_i \boldsymbol{\theta} + W' \end{aligned}$$

where the scalar  $c$  is an intercept and  $e$  is a vector of ones. The covariance of the equation error was developed in [4]:  $R^{(i)} = E [W' W'^T] = R + q^{(i)} \cdot I_N$ , where  $R$  is the equation error covariance matrix and  $q^{(i)}$  reflects the strength of the nonlinearity in the nonlinear observation relation  $h$ . The significant factors that influence the quality of parameter estimation are  $T$ ,  $\Delta T$ , and the geometry of the projectile trajectory relative to the radar.

The augmented parameter estimate

$$\hat{\boldsymbol{\theta}}^{(i+1)} = (\mathbf{H}_i^T R^{(i)-1} \mathbf{H}_i)^{-1} \mathbf{H}_i^T R^{(i)-1} [Z + H_i \hat{\theta}^{(i)} - h(\hat{\theta}^{(i)})] \quad (8)$$

where  $i = 0, 1, \dots$ ; the derivation is given in the Appendix. As  $i$  increases and  $\|\hat{\boldsymbol{\theta}}^{(k+1)} - \hat{\boldsymbol{\theta}}^{(k)}\|$  decreases, the magnitude of the tuning parameter  $q^{(i)}$  is reduced. After convergence is achieved, one can verify that the intercept estimate  $\hat{c}^{(i)}$  is small. Also, after convergence is achieved, one calculates the predicted estimation error covariance  $P = (H^T R^{-1} H)^{-1}$ .

Near the point of convergence, the parameter  $\hat{\theta}$  does not change much. This is in stark contrast to the initial iterations. Thus, initially, the effects of the nonlinearity are pronounced (i.e., the truncation error  $c \neq 0$ ). Hence, to assist convergence for the nonlinear regression with intercept case, the block diagonal terms of the covariance  $R$  in (6) were doubled for early iterations. As the iteration continues to 12 iterations, the extra uncertainty weighting is gradually reduced to one.

Consider the development of (7). If one were to set up a linear regression based on one measurement equation only,  $c$  would be a scalar and  $e$  would consist of a  $N$  vector of ones. Hence, when setting up a nonlinear regression formed from scalar measurements recorded over time, one can think of an average truncation error via the intercept  $c$ , and some additional random error:

$$\begin{bmatrix} c_1 \\ c_2 \\ \vdots \\ c_N \end{bmatrix}_{N \times 1} = c \cdot e + W \quad (9)$$

One should incorporate a separate intercept for each measurement equation. Thus, for the estimation problem we are considering, a separate intercept should apply for the range, azimuth, and elevation in the respective observation relations, namely the parameter

$$c = \begin{bmatrix} c_R \\ c_\phi \\ c_\theta \end{bmatrix}_{2 \times 1} \quad \text{and} \quad e = \begin{bmatrix} e_R & o & o \\ o & e_\phi & o \\ o & o & e_\theta \end{bmatrix}_{3N \times 3}$$

Disappointing estimation performance resulted while using two intercepts, one for range and one for elevation. The intercept for the range measurement equation caused the iterative estimation process to converge at an erroneous minimum when realistic noise is included in the measurements.

However, when one considers a generalized intercept that addresses elevation error and neglects any error contribution from range and azimuth, the estimation process for the nonlinear regression with intercept greatly improves. Specifically, the vector  $e$  then is

$$e = \begin{bmatrix} 0 \\ \vdots \\ 0 \\ \dots \\ 1 \\ \vdots \\ 1 \end{bmatrix}_{2N \times 1}$$

In effect, this includes an intercept to impact the nonlinear elevation measurement equation only.

## VI. ESTIMATION RESULTS

In order to compare the estimation methods, we confine our simulation experiments to a 2-D scenario ( $x, z$  plane). Hence, for the remainder of the paper, we consider the reduced parameter vector:

$$\theta = (x_o, z_o, V_{x_o}, V_{z_o})^T \in \mathbb{R}^4$$

The truth model and measured data vector is generated. The noise on the measurements has zero mean and is Gaussian distributed. The measurement errors reflect current near state-of-the-art hardware accuracy specifications for battle-field radars. Angle and range measurements are assumed independent at each sample and are taken every tenth of a second. At each time increment, the parameter estimate is derived in batch using all previous measurements. Thus, an expanding data window is used. The scenario considers an enemy opposition that is launching unguided artillery shells from an unknown location. Hence, to start the iteration process for each successive batch, we derive the initial parameter guess entirely from measurement observations.

### A. Example 1: Radar Overflight

This scenario demonstrates the major benefits of the novel ILS algorithm augmented with an intercept, compared to standard ILS. By overflying the radar and landing just beyond its location, the geometry causes the nonlinearity in the incoming projectile's elevation angle measurement equation to strengthen. (See Figure 2.) The ballistic coef-

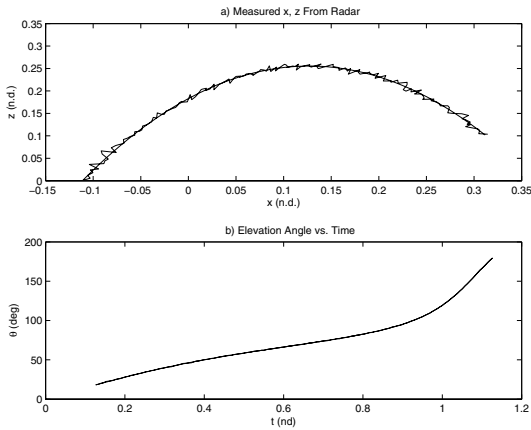


Fig. 2. Typical Ballistic Trajectory. a) Truth model position and measured position. b) Shows a large excursion in  $\theta$ , which accentuates the nonlinearity.

ficient associated with this projectile is relatively large at  $c_b = 1.35$ , which further accentuates the nonlinearity in the  $\theta$  measurement equation. The projectile is fired from the same elevation as the radar and target; however, there is a 0.127 nondimensional time unit delay in initiating radar

measurements. Measurement errors are  $\sigma_\theta = 0.3$  degrees and  $\sigma_R = 10$  meters, respectively.

As one can see from Figures 3 through 4, standard ILS diverges when 80 or more data increments are considered, corresponding to the first 0.506 nondimensional time units of the data (from .127 to .633 nondimensional time units of projectile flight). This results directly from neglecting the

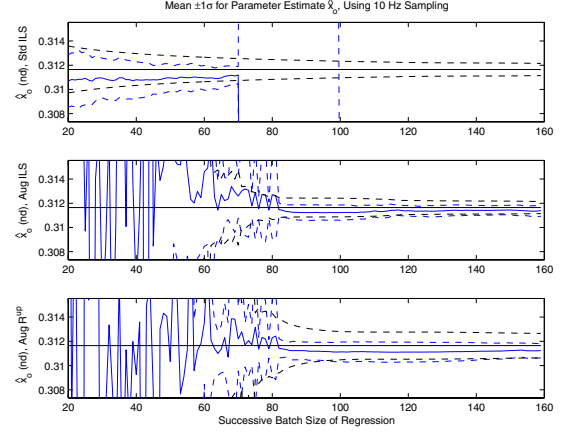


Fig. 3. Result of 20 Monte Carlo runs for strongly nonlinear case. Shows the position parameter estimate,  $\hat{x}_o \pm$  the experimentally determined  $1\sigma$  (blue). Shows  $x_{true} = 0.3116 \pm 1\sigma$  determined from  $R$  (black).

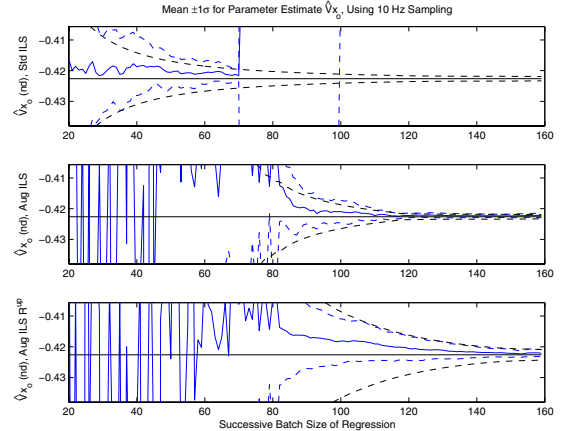


Fig. 4. Result of 20 Monte Carlo runs for strongly nonlinear case. Shows the velocity parameter estimate,  $\hat{V}_{x_o} \pm$  the experimentally determined  $1\sigma$  (blue). Shows  $V_{x_{true}} = -0.4226 \pm 1\sigma$  determined from  $R$  (black).

nonlinearity in the elevation angle measurement equation. Interestingly, the augmented ILS case with generalized intercept requires approximately 65 measurements (from .126 to .538 nondimensional time units of projectile flight) for convergence to the true position parameter and true velocity parameter respectively. Increasing the covariance  $R$  causes slower convergence to the true parameter values, as expected. The bottom line is that a relation exists between the nonlinearity and the measurement noise level. Engagement geometry may dictate using the more sophisticated augmented ILS with intercept algorithm, particularly as

the strength of the nonlinearity increases compared to the measurement noise level.

At this point, we acknowledge that we are really interested in the projectile launch point estimate. Up until this point, we have determined parameter estimates corresponding to the beginning of the batch. One of batch regression's main advantages when compared to sequential (i.e. Kalman Filtering) type estimation is that smoothing is not required in order to obtain estimates of a parameter set prior to the first measurement within the batch.

We assume that the launch point elevation is known. We then use our estimate of  $\hat{z}$  and  $\hat{V}_z$ , along with our knowledge of the kinematics, to determine the launch time estimate:

$$\hat{z} = z_o + (\hat{V}_z + C_b \cdot g \cdot \hat{t}) \cdot \hat{t} - \frac{1}{2} \cdot C_b \cdot g \cdot \hat{t}^2 \quad (10)$$

We now show the estimated parameter position  $\hat{x}_L$  projected back in time to the launch point using (10), for 20 Monte Carlo simulations. Figure 5 shows the experimentally determined estimate for each successive batch size. The

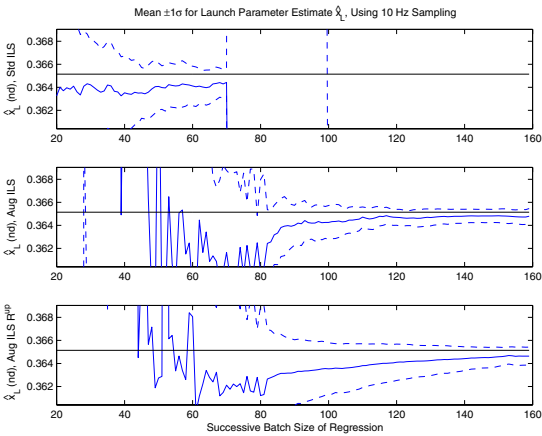


Fig. 5. Result of 20 Monte Carlo Runs. Solid blue lines show the launch position parameter estimate,  $\hat{x}_L \pm$  the experimentally determined  $1\sigma$  dashed lines.  $x_{Ltrue}$  is also shown, in black.

plot also shows the experimentally determined standard deviation of the parameter estimate. If we wanted to show the equation error covariance, we could increase  $R$  to reflect the uncertainty in the time estimate.

### B. Example 2: Stressful Geometry

In this scenario, both the radar and enemy projectile launch location are on hilltops, 1500 meters apart. A projectile is fired towards the radar, but falls short into a ravine separating the two hilltops (Figure 6). Also, there is little movement in elevation angle for the first 120 measurements.

Figures 7 and 8 show the results of the estimation process. The estimation problem is not impacted by the nonlinearity, which is weak compared to the strong measurement noise. Note that  $\sigma_\theta = 0.1$  degrees and  $\sigma_R = 10$  meters. Standard ILS obtains the estimate quickly, after incorporating as few as 10 measurements. All three estimation methods develop a good estimate by  $\sim 90$  data increments.

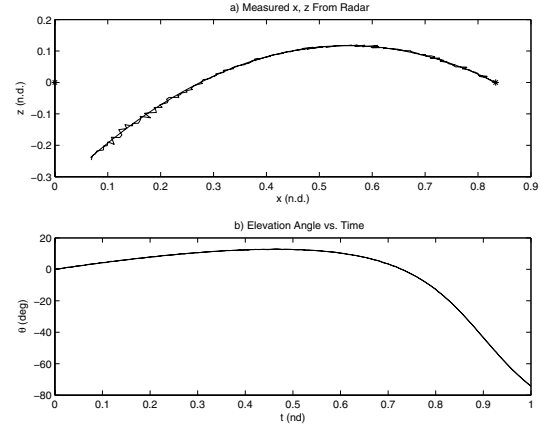


Fig. 6. Second Example of Typical Monte Carlo Ballistic Trajectory Profile. a) Shows the truth model position, as well as the position measurements. \* indicates the artillery position and the radar location. b) Shows little movement in  $\theta$  for the first  $\sim 75\%$  of the tracked projectile flight.

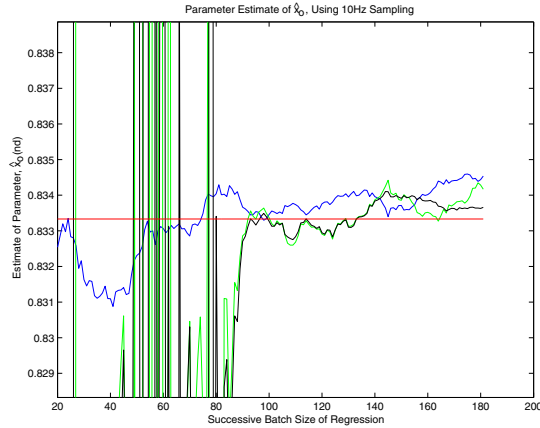


Fig. 7. Position estimate, as provided by a typical Monte Carlo Run with near linear changes in elevation. Standard ILS quickly renders a good estimate (blue line). The augmented ILS with intercept (green line) and the augmented ILS estimate determined with increased uncertainty in  $R$  (black line) also produce good estimates after  $\sim 90$  measurements.

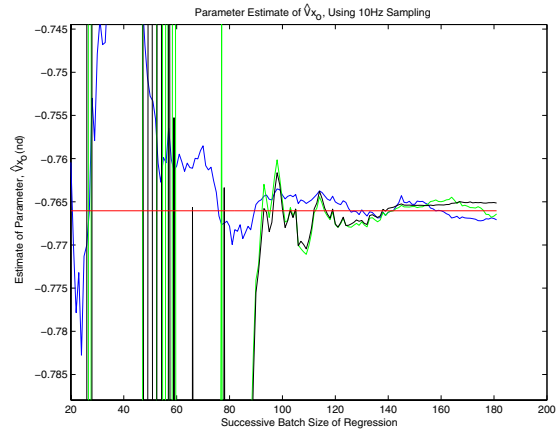


Fig. 8. Velocity Estimate of a typical Monte Carlo Run with near linear changes in elevation. Line types are the same as in Figure 7.

The delay in the augmented ILS estimation process is caused by the “lack” of information in the elevation measurement, as the elevation measurement moves little from  $0^\circ$  for the first 0.8 nondimensional time units of projectile flight (Figure 6). Recall that the intercept is allowed to float unconstrained throughout the iteration process. This causes the increased estimate convergence time when compared to Example 1, even though the elevation measurement noise statistics are greatly enhanced in the latter example. Most importantly, note that after data is accumulated for 0.444 nondimensional time units, the augmented ILS with generalized intercept does not hurt the estimate.

Finally, the best  $\hat{x}$  position estimate is obtained when the block diagonal terms of the covariance matrix  $R$  are slightly increased and one uses  $\sim 140$  or more measurements in the batch. The estimates were generated with the covariance block diagonal terms at 25% above their typical level. The estimates are quite invariant compared to their counterparts when the batch size contains at least 140 data points. The final  $\sim 40$  data points correspond to the last four seconds of the projectile flight. The geometry in Example 2 accentuates two effects in the observations, as the elevation angle begins to change rapidly, corresponding to the projectile crashing into the ravine. First, the measurement errors can cause quite erratic “movement” in the ballistic projectile’s final decent. The added uncertainty to the diagonal terms deemphasizes this erratic movement in the measurement data. (See Figure 6a.) Second, this increase in uncertainty accounts for equation error  $w_{nl}$  previously neglected, as shown in (9). Hence, the additional uncertainty reduces the impact of the nonlinear dynamics that were linearized during the estimation process.

### C. Discussion

These examples demonstrate the range of possible geometry scenarios that an estimation algorithm must deal with. The importance of the relation between the strength of the nonlinearity and measurement noise is explored. Augmented ILS with generalized intercept clearly expands the operational envelope of these batch estimation algorithms. Most importantly, the enhanced augmented estimation method does not adversely impact the estimation ability in the nearly linear estimation cases, if the batch estimation algorithm is given enough measurements. Finally, the parameter estimate may benefit by artificially increasing the block diagonal terms of the covariance matrix  $R$ , a standard Kalman Filter “tuning” process.

## VII. CONCLUSIONS AND EXTENSIONS

### A. Conclusions

We are employing batch data processing and nonlinear regression, augmented with an intercept, and we demonstrate the novel algorithm in a ballistic trajectory tracking scenario. We improve on the estimation performance of standard ILS by incorporating two key features. First, we recognize that the intercept is a multi-variable parameter.

Each nonlinear measurement equation provides an opportunity to introduce a scalar intercept. In our case, the best estimation results are obtained when the intercept is only applied to the critical angle measurement equation where the nonlinearity is strongest. Indeed, the method is extremely effective in cases where the magnitude of the nonlinearity is large compared with the measurement noise level. In addition, the method does not adversely impact the estimation for nearly linear cases, if given enough measurements within the batch. Second, we recognize that when one linearizes a nonlinear system, there is increased uncertainty above and beyond the equation error caused by measurement noise. Hence, “tuning” by increasing the diagonal terms of the equation error covariance matrix  $R$  assists estimation convergence, particularly when problem geometry amplifies the deleterious effects of nonlinearity.

### B. Future Work

The impact of the following on the estimation process is of great interest: signal to noise ratio, geometric dilution of precision of measurement arrangement, number of data points available, physical duration of data record, sampling rate, and the size of the parameter vector  $\theta$ . Finally, the benefits relating to estimation performance afforded by including prior information on the muzzle velocity, require investigation.

## VIII. ACKNOWLEDGMENTS

We thank Professors Peter Maybeck and Mark Oxley, and Dr. Andrew Sparks for their continued insightful advice on issues pertaining to this research. Their insights on the potential need for intercept generalization were invaluable for this paper.

## APPENDIX

### NONLINEAR REGRESSION AUGMENTED WITH AN INTERCEPT

Consider the solution of the augmented linear regression shown in (8) and restated here.

$$\hat{\theta}^{(i+1)} = (\mathbf{H}_i^T R^{-1} \mathbf{H}_i)^{-1} \mathbf{H}_i^T R^{-1} [Z + H_i \hat{\theta}^{(i)} - h(\hat{\theta}^{(i)})]$$

where the iteration counter is  $i = 0, 1, \dots$ . Expanding the aforementioned equation, we observe that

$$\begin{pmatrix} \hat{\theta}^{(i+1)} \\ \hat{c}^{(i+1)} \end{pmatrix} = \begin{bmatrix} H_i^T R^{-1} H_i & H_i^T R^{-1} e \\ e_i^T R^{-1} H_i & e_i^T R^{-1} e \end{bmatrix}^{-1} \begin{pmatrix} H_i^T R^{-1} \\ e_i^T R^{-1} \end{pmatrix} [z + H_i \hat{\theta}^{(i)} - h(\hat{\theta}^{(i)})]$$

We shall require

### Lemma

$$\begin{pmatrix} A & b \\ b^T & \alpha \end{pmatrix}^{-1} = \begin{pmatrix} X & x \\ x^T & \xi \end{pmatrix}$$

where

$$\begin{aligned} X &= \left( A - \frac{1}{\alpha} bb^T \right)^{-1} \\ x &= (bb^T - \alpha A)^{-1} b \\ \xi &= \frac{1}{\alpha} \left[ 1 - b^T (bb^T - \alpha A)^{-1} b \right] \end{aligned}$$

This assumes that  $A$  is symmetric and invertible and that  $(A - \frac{1}{\alpha} bb^T)$  is invertible. Recall that  $\alpha$  and  $\xi$  are scalars.

Proof

$$\begin{pmatrix} A & b \\ b^T & \alpha \end{pmatrix} \begin{pmatrix} Xx \\ x^T \xi \end{pmatrix} = \begin{pmatrix} I & 0 \\ 0 & 1 \end{pmatrix}$$

This implies that

$$AX + bx^T = I \quad (11)$$

$$Ax + \xi b = 0 \quad (12)$$

$$b^T X + \alpha x^T = 0 \quad (13)$$

$$b^T x + \alpha \xi = 1 \quad (13)$$

(13) implies that

$$\xi = \frac{1 - b^T x}{\alpha} \quad (14)$$

Using (12) and (14), we learn that

$$x = (bb^T - \alpha A)^{-1} b \quad (15)$$

Next, consider (14) and (15)

$$\xi = \frac{1}{\alpha} \left[ 1 - b^T (bb^T - \alpha A)^{-1} b \right]$$

Finally, consider (11) and (15)

$$\begin{aligned} AX &= I - bb^T (bb^T - \alpha A)^{-1} \\ &= I - bb^T (bb^T - \alpha A)^{-1} \\ &= I - \alpha A (bb^T - \alpha A)^{-1} + \alpha A (bb^T - \alpha A)^{-1} \\ &\quad - bb^T (bb^T - \alpha A)^{-1} \\ &= I - \alpha A (bb^T - \alpha A)^{-1} + (\alpha A - bb^T) (bb^T - \alpha A)^{-1} \\ &= I - \alpha A (bb^T - \alpha A)^{-1} - I \\ &= -\alpha A (bb^T - \alpha A)^{-1} \\ &= A \left( A - \frac{1}{\alpha} bb^T \right)^{-1} \end{aligned}$$

Hence,

$$X = \left( A - \frac{1}{\alpha} bb^T \right)^{-1}$$

Using the substitutions:  $A = H_i^T R^{-1} H_i$ ,  $b = H_i^T R^{-1} e$ , and  $\alpha = e^T R^{-1} e$ , the Lemma yields

$$\begin{bmatrix} H_i^T R^{-1} H_i & H_i^T R^{-1} e \\ e_i^T R^{-1} H_i & e_i^T R^{-1} e \end{bmatrix}^{-1} = \begin{bmatrix} ULHS & URHS \\ LLHS & LRHS \end{bmatrix}$$

where

$$\begin{aligned} ULHS &= [H_i^T R^{-1} (R - \frac{1}{e^T R^{-1} e} ee^T) R^{-1} H_i]^{-1} \\ URHS &= - [H_i^T R^{-1} (\frac{R}{e^T R^{-1} e} - ee^T) R^{-1} H_i]^{-1} H_i^T R^{-1} e \\ LLHS &= -e^T R^{-1} H_i [H_i^T R^{-1} (\frac{R}{e^T R^{-1} e} - ee^T) R^{-1} H_i]^{-1} \\ LRHS &= \frac{1}{e^T R^{-1} e} + (\frac{1}{e^T R^{-1} e})^2 e^T R^{-1} H_i \\ &\quad [H_i^T R^{-1} (R - \frac{1}{e^T R^{-1} e} ee^T) R^{-1} H_i]^{-1} H_i^T R^{-1} e \end{aligned}$$

Finally, this yields the closed form estimation algorithm

$$\begin{aligned} \hat{\theta}^{(i+1)} &= ([H_i^T R^{-1} (R - \frac{1}{e^T R^{-1} e} ee^T) R^{-1} H_i]^{-1} H_i^T \\ &\quad - [H_i^T R^{-1} (\frac{R}{e^T R^{-1} e} - ee^T) R^{-1} H_i]^{-1} \cdot \\ &\quad H_i^T R^{-1} ee^T) R^{-1} [Z + H_i \hat{\theta}^{(i)} - h(\hat{\theta}^{(i)})] \\ \hat{c}^{(i+1)} &= e^T R^{-1} (I [\frac{1}{e^T R^{-1} e} + (\frac{1}{e^T R^{-1} e})^2 e^T R^{-1} H_i \cdot \\ &\quad [H_i^T R^{-1} (R - \frac{1}{e^T R^{-1} e} ee^T) R^{-1} H_i]^{-1} H_i^T R^{-1} e] \\ &\quad - H_i [H_i^T R^{-1} (\frac{1}{e^T R^{-1} e} R - ee^T) R^{-1} H_i]^{-1}) \\ &\quad \cdot [Z + H_i \hat{\theta}^{(i)} - h(\hat{\theta}^{(i)})] \end{aligned}$$

where  $i = 0, 1, \dots$

## REFERENCES

- [1] J. Buffington, P. Chandler, and M. Pachter, "Integration of On-line System Identification and Optimization-based Control Allocation", AIAA 98-37178, *American Institute of Aeronautics and Astronautics*, 1998, pp. 1746-56.
- [2] M. Pachter, "Stochastic Modeling Based DGPS Estimation Algorithm", *Proceedings of the 39th IEEE Conference on Decision and Control*, Sydney, Australia, December, 2000, pp. 5192-97.
- [3] P. Chandler, M. Pachter, M. Mears and S. Sheldon, "Regression Techniques for Aircraft Parameter Identification from Noisy Measurements in Maneuvering Flight", *Proceedings of the 31st Conference on Decision and Control*, Tucson, Arizona, December, 1992, pp. 2311-16.
- [4] Eric Nelson and Meir Pachter, "Linear Regression with Intercept", AIAA 2004-4757, *AIAA Guidance, Navigation, and Controls Conference*, Providence, RI, August, 2004.
- [5] "U.K. gets Battlefield Radar", *Defense News*, February 2004, p. X.
- [6] William E. Wiesel, *Modern Methods of Orbit Determination*, AFIT, lecture notes, 1998.
- [7] Meir Pachter and Eric Nelson, "Parameter Space Augmentation for Nonlinear System Identification", *Submitted for publication to the IEEE Journal of Automatic Control*, 2004.

□